Glycation-lowering compounds inhibit ghrelin signaling to reduce food intake, lower insulin resistance, and extend lifespan.

Lauren Wimer[1A], Kiyomi R. Kaneshiro[1A], Jessica Ramirez[1], Neelanjan Bose[1], Martin Valdearcos[2], Muniesh Muthaiyan Shanmugam[1], Dominique O. Farrera[3], Parminder Singh[1], Jennifer Beck[1], Durai Sellegounder[1], Lizbeth Enqriquez Najera[1], Lisa Ellerby[1], Soo-Jin Cho[4], John C. Newman[1], James Galligan[3], Suneil Koliwad[2], Pankaj Kapahi[1]*[*]

[1] Buck Institute for Research on Aging, Novato, CA 94949
[2] The Diabetes Center, University of California San Francisco, San Francisco CA 94143
[3] University of Arizona, Tucson, AZ
[4] Surgical Pathology, University of California San Francisco, San Francisco CA 94143
[A] Authors contributed equally
* To whom correspondence should be addressed

Author contributions: PK, SK, JG, JCN, LE involved in conceptualization and supervision. LW, KK, PK, LE, JCN drafted the manuscript. LW, KK involved in analysis and visualization. JR, NB, MV, MMS, DF, PS, JB, DS, LEN involved in experimental procedure, live animal experimentation. SJC involved in blinded pathological assessment. JG and DF involved in experimental quantification and analysis of α-dicarbonyls. All authors have read and agreed to the final version of the manuscript.

Acknowledgements: We thank A. Bartke and D. Medina for discussion and experimental procedure development. B. Schilling, S. Melov for useful discussion. A. Lopez-Ramirez for brain dissections and contribution to the work. C. Patterson for contribution to cohort husbandry and experimentation. We thank the Kapahi Lab at Buck Institute for helpful discussion and critique. We thank the employees of the Phenotyping Core and Morphology Core at the Buck Institute.

Funding statement: We acknowledge support from National Institute of Health: T32AG000266-23 (KK), R01AG038688 (PK), AG045835 (PK), and the Larry L. Hillblom Foundation (PK).

Conflict of interest statement: Lauren Wimer, Neelanjan Bose, and Pankaj Kapahi are patent holders of GLYLO™, a supplement licensed to Juvify Bio by the Buck Institute. Dr. Pankaj Kapahi is the founder of Juvify Bio. The remaining authors have no conflicts of interest to declare.

Data availability: The data that supports the findings of this study are available from the corresponding author upon reasonable request.

Inclusion and diversity: We support inclusive, diverse, and equitable conduct of research.

Graphical Abstract:

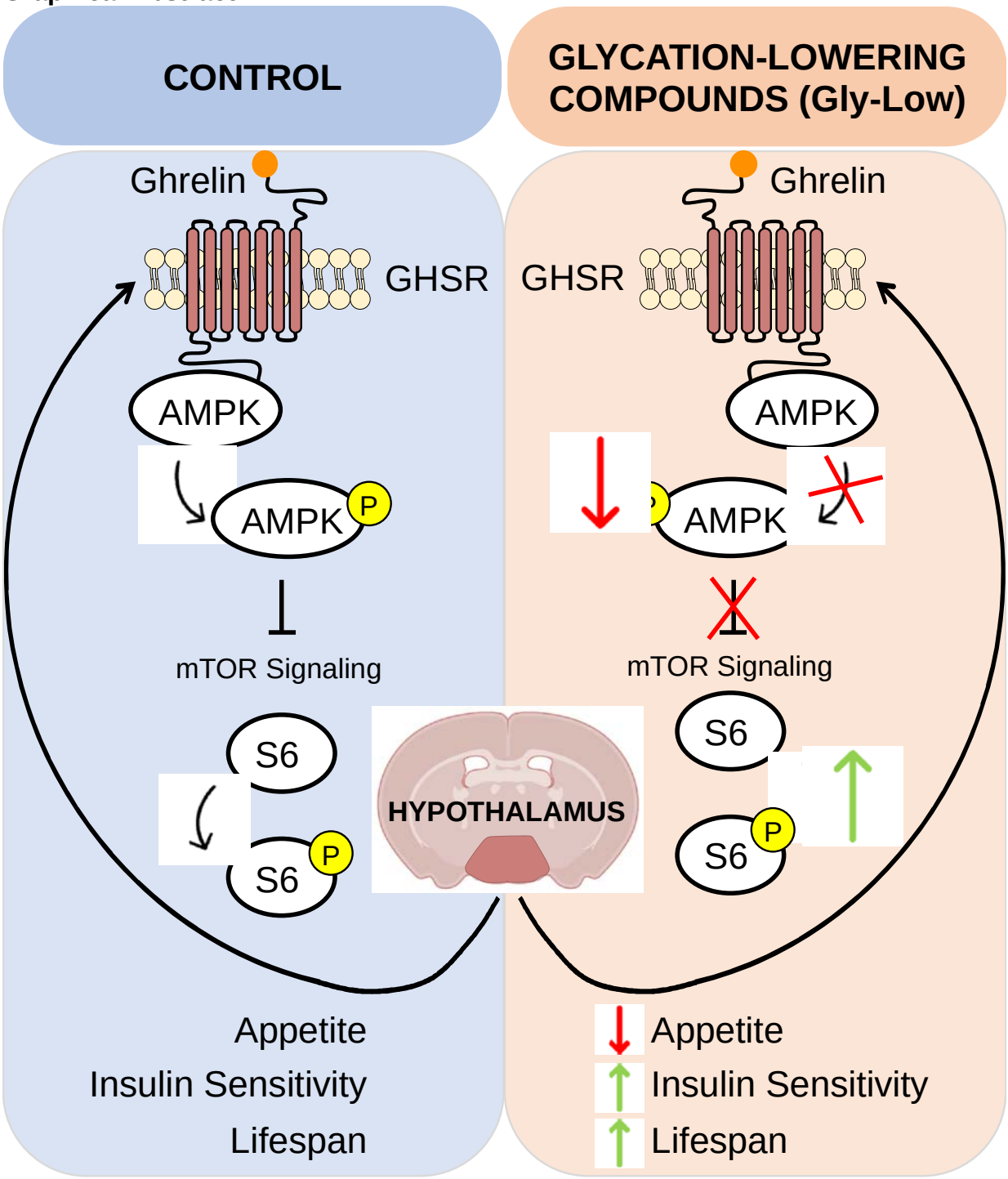

Summary:
Non-enzymatic reactions in glycolysis lead to the accumulation of methylglyoxal (MGO), a reactive precursor to advanced glycation end-products (AGEs), which has been hypothesized to drive obesity and aging-associated pathologies. A combination of nicotinamide, lipoic acid, thiamine, pyridoxamine, and piperine (Gly-Low), was identified to lower glycation by reducing MGO and MGO-derived AGE, MG-H1, in mice. Administration of Gly-Low reduced food consumption, lowered body weight, improved insulin sensitivity, and increased survival in both leptin receptor-deficient ($Lepr^{db}$) and wild-type C57B6/J mice. Unlike caloric restriction, Gly-Low modulated hypothalamic signaling by upregulating mTOR pathway signaling to inhibit ghrelin-mediated hunger response. Gly-Low also slowed hypothalamic aging and increased survival when administered as a late-life intervention, suggesting its potential benefits in ameliorating age-associated decline by inducing voluntary caloric restriction and reducing glycation.

Keywords: aging, methylglyoxal, obesity, diabetes, ghrelin, leptin, hypothalamus, glycation, lifespan

Introduction

Despite the substantial efforts of public health, the incidence of obesity is growing worldwide. Obesity reduces life expectancy by increasing the risk of several diseases, including diabetes, dementia, cardiovascular diseases, certain cancers, and severe COVID-19[1,2]. These obesity-linked comorbidities are a significant burden to the US healthcare system. Lifestyle changes have gained popularity to combat increasingly sedentary lifestyles and excess caloric intake, but dietary improvements remain challenging for most individuals. For many, increased adiposity drives progressive unresponsiveness to homeostatic cues that normally maintain weight stability, such as the adipokine leptin[3,4]. Leptin resistance, in turn, fuels obesity. Leptin resistance is linked to specific functional deficiencies in the leptinergic melanocortin system within the mediobasal hypothalamus that emerges in response to chronic dietary excess and disrupts homeostatic regulation of food intake[5]

Increases in sugar intake are in part responsible for the obesity epidemic[6]. Food overconsumption and obesity are contributing factors to chronic hyperglycemia and enhanced glycolysis, which increases the production of reactive α-dicarbonyls, such as methylglyoxal (MGO)[7,8]. MGO is an unavoidable byproduct of anaerobic glycolysis and is generated spontaneously when glucose breaks down into dihydroxyacetone phosphate (DHAP) and glyceraldehyde-3-phosphate (G3P). MGO reacts nonenzymatically with biomolecules such as proteins, lipids, and DNA to form advanced glycation end-products (AGEs)[9,10]. These covalent adducts contribute to pathogenesis across several diseases by compromising protein function, forming extracellular crosslinks that disrupt tissue architecture, and modifying lipids and nucleic acids[8]. Cellular protection against AGEs occurs by endogenous glyoxalase enzymes, which detoxify MGO and thereby prevent downstream AGEs formation[7,11]. Given that increased sugar consumption, which drives obesity, is accompanied by enhanced glycolysis and concomitant production of toxic glycolytic byproducts, we hypothesized that detoxification of AGEs may be a viable therapeutic against obesity and its associated pathologies.

Here we describe the impact of a combination of nicotinamide, lipoic acid, thiamine, pyridoxamine, and piperine, which we term Gly-Low for their glycation-lowering ability. Gly-Low reduced appetite and obesity in both leptin receptor-deficient ($Lepr^{db}$) and wild-type C57B6/J mice. In contrast to calorie restriction, Gly-Low upregulated mTOR signaling in the hypothalamus to inhibit ghrelin-mediated hunger responses. In aged wild-type mice, Gly-Low treatment increased lifespan, improved insulin sensitivity, and reversed signatures of hypothalamic aging. These findings demonstrate that compounds that lower glycation can be effective tools for both reducing obesity and overcoming the deleterious effects of aging.

A Natural Compound Screen Identifies Compounds That Reduce Glycation Stress

Advanced glycation end-products (AGEs) are toxic adducts formed when proteins and lipids are exposed to sugar. Hyperglycaemia, as occurs in diabetes, accelerates AGE formation and their accumulation at various sites to play a role in worsening diabetes-associated pathologies such as nephropathy, retinopathy, cardiomyopathy, neuropathy, and vascular injury[12]. Diabetic manifestations, such as peripheral neuropathy and reduced lifespan, have been recapitulated in the *C. elegans glod-4* mutant. [13]. This model lacks the endogenous detoxification pathway responsible for the clearance of MGO, the primary precursor of AGEs. We previously utilized this *glod-4* model to perform a high throughput screen of 640 natural compounds (TimTex, NPL640) to identify interventions able to protect against AGE-associated pathologies and diabetic manifestations. We further tested 11 positive hits from our screen (alpha lipoic acid, nicotinamide, piperine), as well as compounds from relevant glyoxalase-associated literature (thiamine[14] and pyridoxamine[15]) in a mammalian model of glycation stress, as measured by rescuing neurite length retraction of rat dopaminergic (N27) neural cells following exposure to MGO (**Figure S1A**). We found that a combination of five compounds: alpha lipoic acid, nicotinamide, piperine, pyridoxamine, and thiamine termed Gly-Low, conferred better protection against MGO relative to the single compounds (**Figure S1B**).

Due to the effectiveness of Gly-Low to protect against glycation-induced stress *in vitro*, we sought to translate this treatment in the context of obesity and hyperglycemia using a diabetic (*Lepr*^{db}) mouse model. This model is ideal to test our glycation-lowering compounds because these mice rapidly develop obesity, hyperglycemia, and glucose intolerance phenotypes that are accompanied by increases in glycation precursors and their adducts in several diabetes-relevant tissues such as the kidneys, heart, and liver[16]. We treated 8-week-old male *Lepr*^{db} mice with a regular, low-fat diet consisting of Gly-Low compounds for 16 weeks (Figure 1). To test the ability of Gly-Low to lower glycation burden, we performed LC/MS analysis on the plasma of mice fed either a Gly-Low supplemented or control diet for 16 weeks and found that Gly-Low significantly lowered the glycolytic metabolite, MGO (61.2% decrease), as well as its protein-bound arginine adduct, MG-H1 (41.45%) (**Figure 1A**).

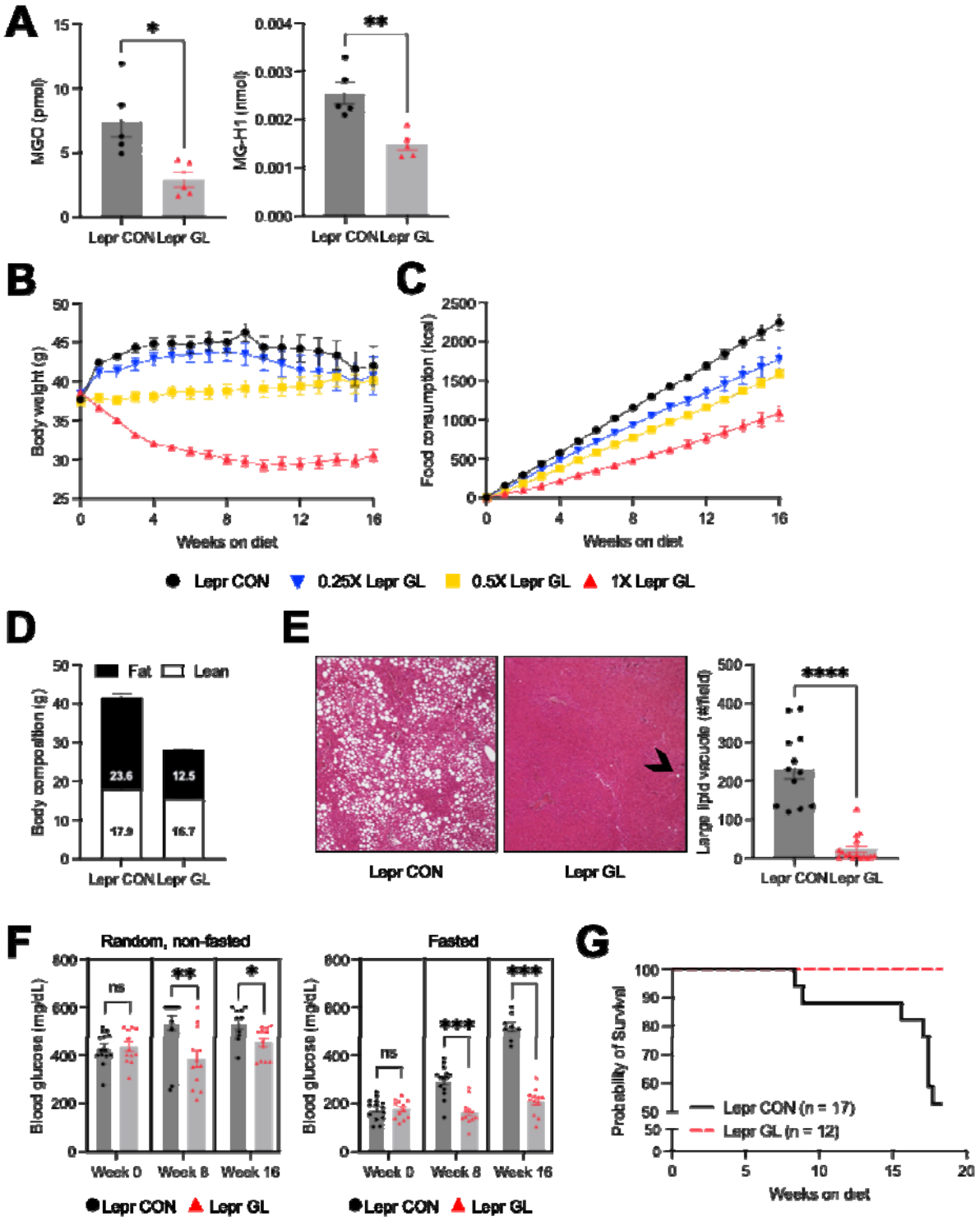
A
MGO (pmol)
MG-H1 (nmol)
Lepr CON
Lepr GL
B
Body weight (g)
Weeks on diet
C
Food consumption (kcal)
Weeks on diet
Lepr CON
0.25X Lepr GL
0.5X Lepr GL
1X Lepr GL
D
Fat
Lean
Body composition (g)
23.6
12.5
17.9
16.7
Lepr CON
Lepr GL
E
Lepr CON
Lepr GL
Large lipid vacuole (#/field)
F
Random, non-fasted
Fasted
Blood glucose (mg/dL)
Week 0
Week 8
Week 16
ns
Lepr CON
Lepr GL
G
Probability of Survival
Lepr CON (n = 17)
Lepr GL (n = 12)
Weeks on diet

Figure 1: Glycation-lowering compounds (Gly-Low) lower glycolytic byproducts as well as rescue hyperphagia and obesity-associated pathologies in a diabetic, leptin receptor deficient (*Lepr*^{db}) mouse model.
A) Levels of glycolytic byproduct, MGO (left), and its arginine adduct, MG-H1 (right), were reduced in the plasma of male mice treated with Gly-Low. n = 5 per treatment group, measured by LC/MS. B) Gly-Low had a dose-dependent effect on body weights of male *Lepr*^{db} mice fed varying concentrations of Gly-Low over a 16-week experimental timeline. n = 12 per treatment group (n = 17 in the control group). C) Cumulative food consumption rates (kcal) were altered in a dose-dependent manner with varying concentrations of Gly-Low treatment. n = 3 cages of group-housed animals per treatment (n = 5 in the control group). D) Decreases in absolute fat and lean mass of Gly-Low treated mice compared to their controls. n = 12 (Gly-Low, in duplicate), n = 8 (Control, in duplicate). E) Representative images of H&E stained liver sections showing the presence of large lipid vacuoles (black arrow) of control fed and Gly-Low fed mice and bar graph quantification. n = 4 livers per treatment group, 4 fields of view per animal. F) Random (non-fasted) and fasted (16h) blood glucose levels up to a max of 600 mg/dL*. n = 12 per treatment group (n = 17 in the control, with deaths throughout the study [1 death before 8 weeks, 8 deaths before 16 weeks]). *Handheld Accucheck glucometer had a maximum read capacity of 600 mg/dL. Therefore, any values above max read capacity were listed as 600 mg/dL. G) Survival curves of control mice and Gly-Low fed mice prior to their experimental endpoint. p = 0.0070 (log-rank Mantel-Cox), p = 0.0076 (Gehan-Breslow-Wilcoxon). Significance: ns (not significant), * $p < 0.05$, ** <0.005, *** <0.0005). Statistical analyses performed by unpaired T-test.

Glycation-Lowering Compounds (Gly-Low) Reduces Food Intake and Diabetic Pathologies in *Lepr*^{db} Mice

We found that Gly-Low had a dose-dependent effect on the body weights of mice fed over a 16-week experimental timeline (**Figure 1B**). By 8 weeks of age, *Lepr*^{db} mice are already overweight (Jackson Laboratories). During the treatment period, control-fed *Lepr*^{db} mice continued to gain body weight reaching a group average of 45 grams by 8 weeks, which is roughly 50% more than that of an average wild-type mouse and represents a state of extreme obesity (Jackson Laboratories). In contrast, by 8 weeks on the highest concentration of Gly-Low supplemented diet, *Lepr*^{db} mice lost an average of 22% from their starting body weights, reaching a group average of 30 grams, which is roughly the average weight of wild-type (C57B6/J) male mice at that age (Jackson Laboratories) (**Figure 1B**). This weight was maintained over the remainder of the experimental time course. We found that the weight loss of Gly-Low treated mice was primarily due to reduced food consumption and not due to changes in energy expenditure or activity levels (**Figure S2A-S2B**) or due to food aversion (**Figure S3A-S3F**). Given their reduced food intake, we performed several tests to rule out food aversion. Administration methods for Gly-Low were adjusted for intraperitoneal (IP) injection and food consumption rates were similarly decreased (**Figure S3A-S3B**). Fasted mice (18h) were not resistant to a reintroduced Gly-Low diet (**Figure S3C-S3D**). Additionally, Gly-Low did not diminish food intake when incorporated into a highly palatable high-fat diet (**Figure S3E-S3F**). Together these experiments support the notion that Gly-Low inhibits food intake without causing food aversion. Gly-Low's efficacy to induce voluntary caloric restriction may be dependent on dietary composition as it failed to reduce food intake in a high-fat diet.

In summary, dietary Gly-Low treatment prevented the hyperphagic phenotype characteristic of *Lepr*^{db} mice, which at the highest concentration reduced average daily food intake by 52% (~72 kcal/day) relative to control-fed mice for the 16-week treatment period (**Figure 1C**). Due to its effectiveness, we chose to restrict further *in vivo* analyses to the highest dosage of Gly-Low supplementation which provided robust changes in weight and MGO levels.

To test the ability of Gly-Low to reduce obesity and diabetes-associated pathologies, we assessed mice for improvements in body composition, liver adiposity, and glucose regulation. Dual x-ray absorptiometry (DXA) analysis, an assay for the direct calculation of fat and bone mass, indicated that Gly-Low treated mice had a 46.9% reduction in absolute fat mass and a 15.9% reduction in lean mass (**Figure 1D**). These changes are indicative of a healthier body composition. Consistent with the reduced adiposity observed by DXA analysis, histological analysis revealed an 89.8% reduction in lipid vacuoles in liver samples of treated mice (**Figure 1E**). These changes in fat accumulation indicate that Gly-Low treatment improves the dysregulated lipid homeostasis observed in this mouse model. In agreement with reduced glycation burden, Gly-Low treated mice displayed significantly improved glycemic control as indicated by a 9.9% reduction in fasted glucose and 28.4% reduction in non-fasted (random) blood glucose levels after 8 weeks of treatment that persisted over the entire course of treatment (**Figure 1F**). These observed improvements in glycemic control of Gly-Low fed mice were accompanied by reduced polyurea (**Figure S2C**), measured by weighing home cages to determine cage soiling. Polyurea occurs during diabetes when the kidneys fail to filter out sugar from the urine resulting in excessive urine output. This is largely driven by excessive blood sugar levels. In addition to polyuria, proteinuria, the presence of protein in the urine, is indicative of diabetic kidney damage[17]. We found that control mice had increasing levels of protein in their urine over the experimental time course indicative of worsening kidney function. In contrast, Gly-Low fed mice had reduced protein in their urine (**Figure S2D**), suggesting a protective role within the kidney. The ability of Gly-Low to reduce hyperphagia and diabetes-associated pathologies in male *Lepr*^{db} mice translated to a complete rescue in early mortality rates during the experimental timeline (**Figure 1G**). Previous reports demonstrated that male *Lepr*^{db} mice had a median lifespan of 349 days, with mortality continuously occurring after 16 weeks of age. Consistent with these reports, we observed an 18% decrease in cohort numbers in our control-fed mice by 15 weeks on diet (23 weeks of age)[18]. By the time of dissections (26 weeks of age), control-fed mice had a 52.9% chance of survival, while Gly-Low fed mice had no recorded experimental deaths. Collectively, these findings in a leptin receptor-deficient mouse model highlight the therapeutic potential of Gly-Low in treating various obesity- and diabetes-associated conditions by reducing overconsumption, associated glycation burden, and glycation-associated pathologies.

Gly-Low Reduces Food Intake In a Leptin-Independent Manner

To determine whether Gly-Low reduces food intake in a non-hyperphagic model, we treated wild-type (C57BL/6J) male mice and assessed natural leptin signaling cascades

(Figure 2). Leptin is the hormone responsible for satiety signaling within the hypothalamus, controlling food consumption[19]. As leptin increases and binds the leptin receptor (Lepr), STAT3 becomes phosphorylated in dopaminergic neurons to signal satiety[19]. To investigate whether Gly-Low modulated leptin signaling, we intraperitoneally (IP) injected wild-type mice with exogenous leptin or a vehicle control following acclimation to either a control or a Gly-Low supplemented diet. Gly-Low did not exacerbate or dampen the effects of leptin relative to their vehicle controls as the fold changes in food intake from both treatment groups were comparable (**Figure 2A**). In addition to unchanged feeding behavior in response to leptin, Gly-Low did not statistically alter regional (arcuate nucleus (ARC), ventromedial hypothalamus (VMH), dorsomedial hypothalamus (DMH), posterior hypothalamus (PH)) hypothalamic pSTAT3 signaling (**Figure 2B**). This indicates that Gly-Low reduces food intake independent of the leptin signaling pathway, consistent with our findings in a leptin receptor-deficient model (Figure 1).

As occurred in male *Lepr*^{db} mice, Gly-Low treatment significantly reduced body weights and food consumption in male C57BL/6J mice. Body weights decreased over three weeks after beginning a Gly-Low supplemented diet, then remained stable for the duration of the experiment (a decrease of 13.6%). On the other hand, control-fed mice consistently gained weight, resulting in an average weight of 35 grams by the end of the experiment (an increase of 17.1%) (**Figure 2C**). Food consumption of Gly-Low fed mice was decreased by 19.6% (86.61 kcal/day to 69.77 kcal/day) compared to control-fed mice (**Figure 2D**). Additionally, DXA analysis indicated that wild-type mice fed Gly-Low had a 67.9% reduction in adiposity ($p < 0.0001$) while lean mass only decreased by 11.5%($p = 0.007$) (**Figure 2E**). Similar to improved glucose homeostasis observed in *Lepr*^{db} mice, wild-type mice showed improved glucose tolerance as indicated by glucose tolerance testing (GTT). Following an IP injection of exogenous glucose, Gly-Low fed mice demonstrated a reduced peak in blood glucose levels relative to control-treated mice (47.0% lower maximum blood glucose with a 45.4% lower area under the curve (AUC) value) (**Figure 2F**). Insulin tolerance testing (ITT) was used to determine whether Gly-Low treated mice had a higher sensitivity to injected insulin (2 mg/kg). Insulin had a more robust effect in reducing blood glucose levels in Gly-Low fed mice (62.7% reduction relative to baseline) relative to control mice (33.5% reduction relative to baseline) (**Figure 2G**). Together, these findings indicate that Gly-Low reduces adiposity and improves glucose homeostasis in wild-type mice.

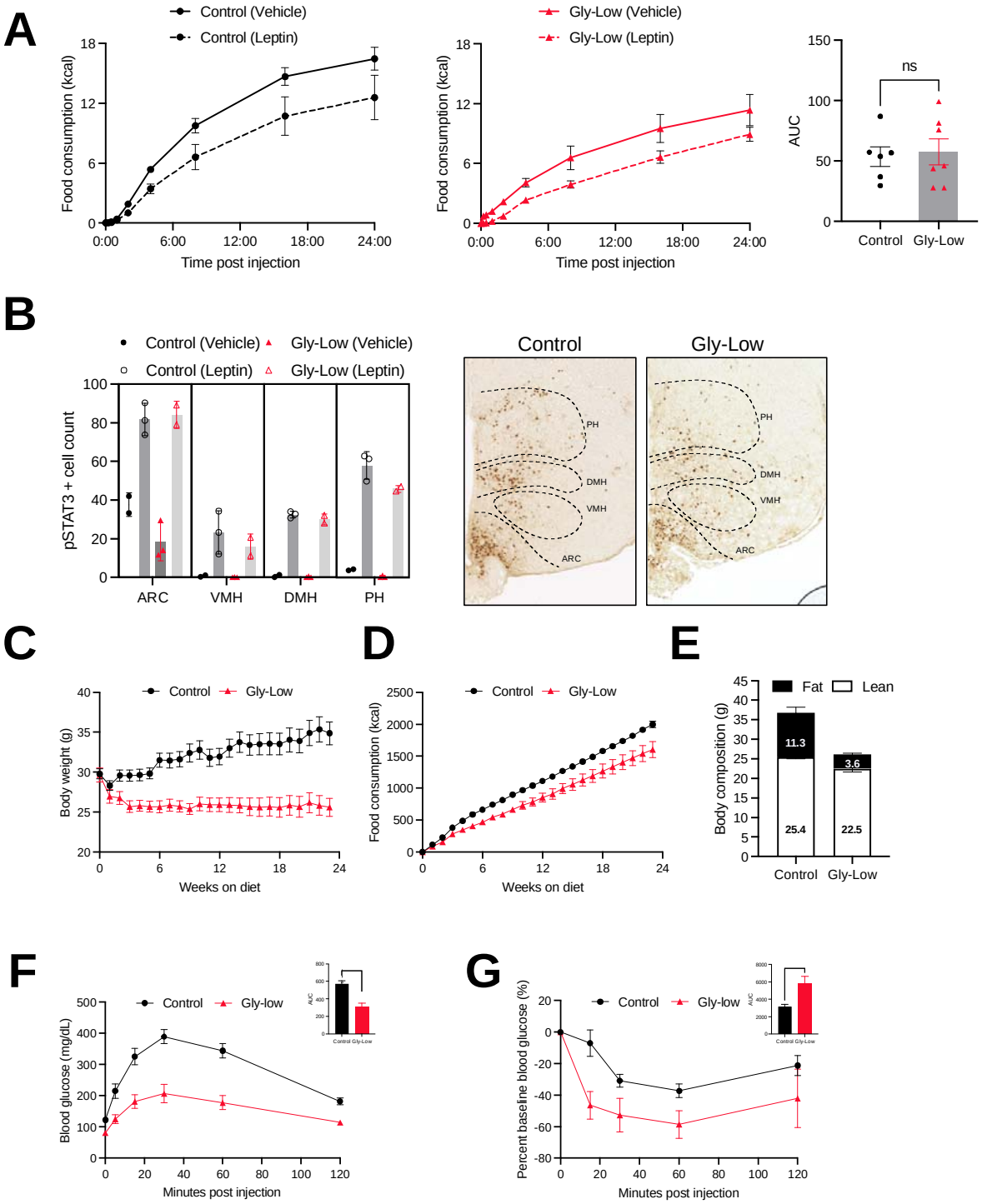
A
Control (Vehicle)
Control (Leptin)
Food consumption (kcal)
Time post injection
Gly-Low (Vehicle)
Gly-Low (Leptin)
AUC
ns
Control
Gly-Low
B
Control (Vehicle)
Gly-Low (Vehicle)
Control (Leptin)
Gly-Low (Leptin)
pSTAT3 + cell count
ARC
VMH
DMH
PH
Control
Gly-Low
C
Control
Gly-Low
Body weight (g)
Weeks on diet
D
Food consumption (kcal)
Weeks on diet
E
Fat
Lean
Body composition (g)
11.3
3.6
25.4
22.5
F
Control
Gly-low
Blood glucose (mg/dL)
Minutes post injection
G
Percent baseline blood glucose (%)
Minutes post injection

Figure 2: Gly-Low works independently of leptin to induce voluntary caloric restriction and improve glucose homeostasis in wild-type C57B6/J mice.
A) Food consumption rates (kcal) of wild-type mice fed a control diet (left, black) or a Gly-Low diet (right, red) were reduced following an injection of leptin compared to those given a saline vehicle control. Area under the curve (AUC) analysis of the change in food consumption demonstrated no change between diets. n = 7 per treatment group. B) pSTAT3 staining patterns in various regions of the hypothalamus following an injection of leptin or a saline vehicle control were similar between control fed and Gly-Low fed wild-type mice (left). n =3 per treatment group. ARC (arcuate nucleus), VMH (ventromedial hypothalamus), DMH (dorsomedial hypothalamus), PH (posterior hypothalamus) Representative image of pSTAT3 positive cells and defined regions of the hypothalamus (right). C) Body weights were significantly reduced in Gly-Low fed mice relative to control fed mice. n = 9 per treatment group. D) Food consumption rates were slightly reduced with Gly-Low treatment. n = 3 grouped housed cages. E) Absolute fat and lean mass of Gly-Low fed mice were significantly lower than control fed mice. n = 9 per treatment group. F) Glucose tolerance testing (GTT) results demonstrated Gly-Low fed mice had lower maximum blood glucose levels relative to control; AUC quantified and demonstrated by bar graph. n = 9. G) Insulin tolerance testing (ITT) results demonstrated Gly-Low mice had larger reductions in blood glucose levels following an injection of insulin relative to control mice; AUC quantified and demonstrated by bar graph. n = 6 per treatment group. Significance: ns $p > 0.05$, * $p < 0.05$, ** <0.005, *** <0.0005). Statistical analyses performed by unpaired T-test.

Gly-Low Reduces Glycolysis and Enhances Cellular Detoxification Pathways in the Hypothalamus

The hypothalamus is aptly positioned at the brain-body interface (third ventricle) to sense circulating nutrients and hormones in the periphery and maintain bodily homeostasis, in part by regulating caloric intake[20,21]. Having established that Gly-Low reduces glycation burden, improves glucose regulation, and reduces food intake, we used an unbiased omics approach to identify pathways altered by Gly-Low treatment in the hypothalamus of wild-type C57BL/6J mice. We assessed changes in hypothalamic transcripts and circulating (plasma) metabolites when wild-type mice were acutely treated (1 week) with a Gly-Low diet (Figure 3). To investigate changes that may explain the ability of Gly-Low to reduce glycation burden, we analyzed genes that generate (glycolysis) or detoxify (cellular detoxification) glycation byproducts. We found that Gly-Low fed mice showed reduced expression of glycolytic genes ($p<0.05$ T-test of observed versus expected (bootstrapped) z-scores) (**Figure 3A**). In contrast, genes responsible for cellular detoxification showed increased expression in Gly-Low fed mice ($P<0.0005$ T-test of observed versus expected (bootstrapped) z-scores) (**Figure 3A**). Consistent with our transcriptome findings, targeted metabolomics data of plasma revealed decreased glycolysis and increased pentose phosphate pathway (PPP) utilization, which regenerates glutathione necessary for MGO-specific and generalized cellular detoxification[22,23] (**Figure 3B**). These findings suggest that Gly-Low may reduce the glycation burden by both reducing its production and enhancing its clearance.

To investigate how Gly-Low may be impacting feeding behavior, we analyzed the 1,407 genes differentially expressed in the hypothalamus of Gly-Low fed vs control-fed mice

for changes to canonical feeding behavior genes. Interestingly, two well-characterized regulators of hunger and satiety, *Agrp* and *Pomc*, were consistently changed in the direction typically observed in hungry mice[24] (**Figure 3C**). *Agrp* and *Pomc*-positive cells are localized within the hypothalamus and are directly inhibited and activated, respectively, by leptin[25,26]. In contrast, *Agrp* and *Pomc* are activated and inhibited, respectively, by ghrelin, a hormone produced in the stomach and sensed by receptors within the hypothalamus[27,28]. While the changes observed in *Agrp* and *Pomc* transcript levels in response to Gly-Low treatment predict activation of ghrelin signaling, ghrelin-associated genes Gh (growth hormone), Ghsr (growth hormone secretagogue receptor), and Ghrhr (growth hormone releasing hormone receptor) were all downregulated (**Figure S4A**).

Gly-Low inhibits Ghrelin Signaling

Given Gly-Low's lack of effect on leptin signaling, we examined whether it influenced circulating levels of the hunger hormone, ghrelin. Ghrelin is a peptide produced in the stomach during fasting and times of hunger[29]. Following production, the circulating hormone binds its receptor, the growth hormone secretagogue receptor (Ghsr)[30] within the hypothalamus to engage signaling pathways that stimulate food intake (Pomc and Agrp)[27,31]. Ghrelin signaling is halted by competitive binding of the ghrelin receptor by liver-derived hormone, LEAP2[32], or when ghrelin production is reduced during feeding in response to endothelial stretching of the stomach[29]. To determine whether Gly-Low affected ghrelin production, we measured levels of acylated ghrelin as well as its endogenous antagonist, LEAP2, in the plasma. We found no significant difference in ghrelin levels between the treatment groups (198.6 pg/mL in the plasma of control-fed mice, 203.9 pg/mL in the plasma of Gly-Low fed mice) (**Figure 3D**). However, LEAP2 levels were significantly decreased in Gly-Low fed mice (56.1 ng/mL vs. 33.5 ng/mL). These changes would predict the activation of appetite promoting pathways counter to what we would expect given the appetite suppressing effect of Gly-Low (**Figure 3E**). Ghrelin signaling stimulates the release of growth hormone (GH)[33], which in turn goes on to stimulate the release of IGF-1 in a well-studied GH/IGF-1 endocrine axis within the hypothalamus and pituitary[34]. To determine if Gly-Low impacts ghrelin signaling, we measured levels of insulin-like growth factor (IGF-1). Surprisingly, IGF-1 levels were decreased in the plasma of Gly-Low fed mice (607.4 ng/mL vs. 543.7 ng/mL), indicative of disrupted ghrelin signaling (**Figure 3F**). To further probe this hypothesis, we subjected control and Gly-Low fed mice to exogenous acylated ghrelin, known to activate ghrelin signaling and thus induce hunger and increase feeding behavior[35]. As expected in control-fed mice, ghrelin-injected mice consumed significantly more food (average of 75% increase) relative to PBS-injected controls post-IP injection (**Figure 3G**). In contrast, Gly-Low fed mice failed to respond to ghrelin injections with increased food consumption (an average of 23% less food consumed relative to PBS-injected controls) (**Figure 3H**). These findings suggest a role for impaired ghrelin signaling in the reduced food intake observed upon Gly-Low treatment.

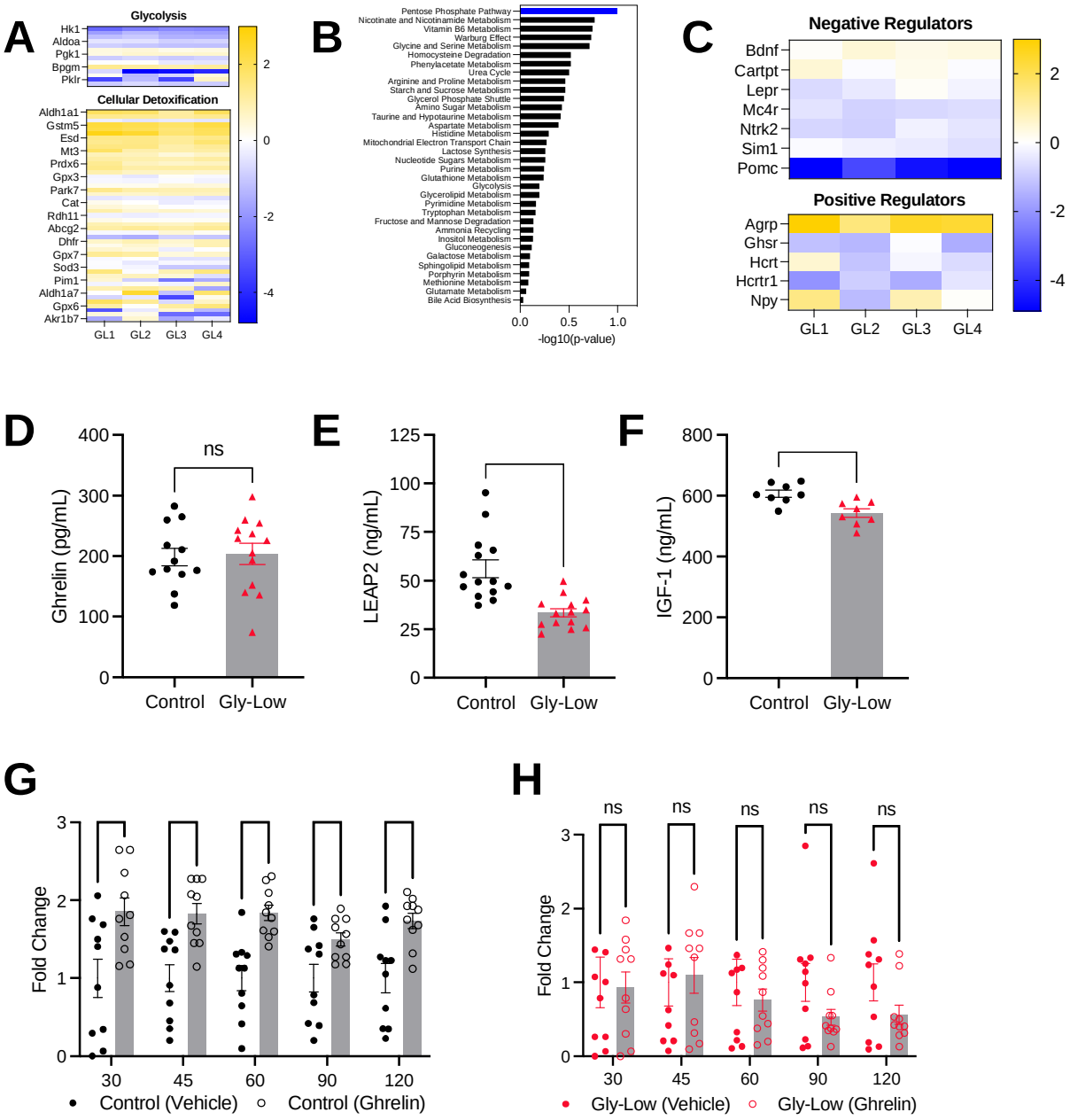
A
Glycolysis
Hk1
Aldoa
Pgk1
Bpgm
Pklr
Cellular Detoxification
Aldh1a1
Gstm5
Esd
Mt3
Prdx6
Gpx3
Park7
Cat
Rdh11
Abcg2
Dhfr
Gpx7
Sod3
Pim1
Aldh1a7
Gpx6
Akr1b7
GL1
GL2
GL3
GL4
2
0
-2
-4
B
Pentose Phosphate Pathway
Nicotinate and Nicotinamide Metabolism
Vitamin B6 Metabolism
Warburg Effect
Glycine and Serine Metabolism
Homocysteine Degradation
Phenylacetate Metabolism
Urea Cycle
Arginine and Proline Metabolism
Starch and Sucrose Metabolism
Glycerol Phosphate Shuttle
Amino Sugar Metabolism
Taurine and Hypotaurine Metabolism
Aspartate Metabolism
Histidine Metabolism
Mitochondrial Electron Transport Chain
Lactose Synthesis
Nucleotide Sugars Metabolism
Purine Metabolism
Glutathione Metabolism
Glycolysis
Glycerolipid Metabolism
Pyrimidine Metabolism
Tryptophan Metabolism
Fructose and Mannose Degradation
Ammonia Recycling
Inositol Metabolism
Gluconeogenesis
Galactose Metabolism
Sphingolipid Metabolism
Porphyrin Metabolism
Methionine Metabolism
Glutamate Metabolism
Bile Acid Biosynthesis
0.0
0.5
1.0
-log10(p-value)
C
Negative Regulators
Bdnf
Cartpt
Lepr
Mc4r
Ntrk2
Sim1
Pomc
Positive Regulators
Agrp
Ghsr
Hcrt
Hcrtr1
Npy
GL1
GL2
GL3
GL4
2
0
-2
-4
D
Ghrelin (pg/mL)
400
300
200
100
0
ns
Control
Gly-Low
E
LEAP2 (ng/mL)
125
100
75
50
25
0
Control
Gly-Low
F
IGF-1 (ng/mL)
800
600
400
200
0
Control
Gly-Low
G
Fold Change
3
2
1
0
30
45
60
90
120
Control (Vehicle)
Control (Ghrelin)
H
Fold Change
3
2
1
0
ns
ns
ns
ns
ns
30
45
60
90
120
Gly-Low (Vehicle)
Gly-Low (Ghrelin)

Figure 3: Gly-Low treatment alters hypothalamic gene expression consistent with reduced glycation and increased hunger but impairs appetite stimulating effects of exogenous ghrelin. A) Heatmaps of glycolysis genes (GO: 0061621) and cellular detoxification genes (GO:199074) in the hypothalamus of Gly-Low fed mice. B) Metabolomics of plasma from mice acutely-treated (1 week) with Gly-Low; the top altered pathway was the Pentose Phosphate Pathway (blue). C) Canonical feeding genes responsible for the negative and positive regulation of feeding were significantly differentially expressed in the hypothalamus of Gly-Low fed mice. D) Plasma levels of ghrelin were unchanged with Gly-Low treatment n = 12-13 per treatment group. E) Plasma levels of LEAP2, the endogenous antagonist of ghrelin, were significantly lower in Gly-Low fed mice. n = 14 per treatment group. F) Plasma levels of IGF-1 were significantly lower in Gly-Low fed mice. n = 8 per treatment group. G) Fold changes in food consumption of ghrelin-injected versus PBS-injected control fed mice and H) Gly-Low fed mice n = 10 per treatment group. Significance: ns $p > 0.05$, * $p < 0.05$, ** <0.005, *** <0.0005). Statistical analyses performed by unpaired T-test.

Gly-Low Impairs Ghrelin Signaling and Increases mTOR Signaling In The Hypothalamus

Given that Gly-Low inhibits hypothalamic ghrelin signaling independent of ghrelin production, we investigated the biochemical changes downstream of the ghrelin receptor (Ghsr) (Figure 4). Activation of the ghrelin receptor, Ghsr, as occurs during fasting, results in the increased phosphorylation of AMPK, which in turn inhibits protein S6 phosphorylation and downstream protein synthesis to preserve energy when nutrient availability is low (**Figure 4A**)[36]. Growth hormones such as IGF-1, bind receptors in the hypothalamus to counteract ghrelin by promoting phosphorylation of AKT. This in turn activates mTOR, subsequent S6 kinase phosphorylation and upregulates protein synthesis in times of surplus nutrient availability (**Figure 4A**)[37]. Our data suggest that there is impaired ghrelin signaling given that protein expression levels of phosphorylated AKT are not elevated in hypothalamic lysates from Gly-Low fed mice (**Figure 4B**). Consistent with impaired ghrelin signaling, hypothalamic lysates from Gly-Low fed mice demonstrate significantly reduced phosphorylated AMPK protein levels and increased phosphorylated S6 protein levels (**Figure 4B**). Consistent with increased levels of phosphorylated S6 protein levels in hypothalamic lysates, upregulated genes of Gly-Low treated mice were most significantly enriched for ribosomal translation and protein synthesis pathways (**Figure 4C**). Another interesting finding from our RNA sequencing analysis was the significant upregulation of genes involved in ATP synthesis (**Figure 4SB**), specifically within the mitochondrial electron transport chain (ETC). We hypothesize this increase in ATP synthesis may serve to fuel increased demands in protein synthesis and homeostasis. Together these experiments suggest that Gly-Low lowers food intake by inhibiting ghrelin signaling.

Hypothalamic Transcripts of Gly-Low Treated Mice Do Not Mimic Those Of Caloric Restriction (CR)

Our studies highlight both similarities and differences between Gly-Low treatment and traditional (enforced) caloric restriction (CR). To further explore differences between the

two interventions, we compared our differentially expressed gene set from the hypothalamus of Gly-Low fed mice with those from publicly available bulk-sequenced hypothalamus of calorically restricted mice[38]. Interestingly, when gene expression fold changes from Gly-Low fed mice were plotted regressed against fold changes from CR-treated mice, we found a significant negative correlation ($p < 0.0001$, $R^2 = 0.3923$, Pearson's correlation) (**Figure 4D**). This suggests that transcriptional changes that occur in the hypothalamus in response to Gly-Low are largely opposite to those that occur in response to CR.

Gly-Low Counters Aging-Associated Changes in Hypothalamic Gene Expression

Hypothalamic inflammation that occurs with aging has been causally linked with whole-body aging phenotypes and age-related metabolic dysfunction[39]. Elevated glycation stress, as occurs with age, drives inflammation in many tissues, including the brain. Therefore, we hypothesized that Gly-Low could reduce inflammation in the hypothalamus of aged mice and thereby preserve youthful hypothalamic signaling and whole-body aging phenotypes. To test this, we profiled the hypothalami of control-fed young (3 months old) mice, control fed aged (25 months old) mice, and Gly-Low fed aged (25 months old) mice. To assess how Gly-Low influences the expression of genes that change with age, we focused on the set of genes for which gene expression is significantly changed both with age (Aged versus Young) and in aged mice fed Gly-Low for five months (Aged Gly-Low vs Aged Control). We found that the changes in gene expression that occur with age are significantly anticorrelated with the changes that occur in aged mice fed Gly-Low ($p < 0.0001$, $R^2 = 0.89$) (**Figure 4E**). To assess the functional impact that these gene expression changes may represent, we performed pathway analysis on the set of genes that are oppositely regulated with age versus with Gly-Low supplementation. Complement activation was the most significantly enriched pathway among genes that are upregulated in the hypothalami of aged control fed mice but downregulated in aged mice fed Gly-Low. Recently, the single-cell analysis identified complement protein C1qa as a marker that distinguishes microglia and macrophages from other cell types in the mouse hypothalamus[40]. In the hypothalamus of aged mice, *C1qa* in microglia, and *C1qa* and *C1qc* in macrophages, are upregulated[40]. Our finding that Gly-Low reduces the expression of these complement proteins in aged mice suggests that Gly-Low may be impacting age-related phenotypes in these cell types more broadly. To explore this, we analyzed the sets of genes that are significantly altered in each cell type of the aged hypothalamus for gene expression changes in our datasets. We found that genes upregulated in macrophages, microglia, and oligodendrocytes with age are significantly downregulated in aged Gly-Low fed mice relative to aged control fed mice (**Figure 4F and Figure S4C-S4E**). Interestingly, genes that are downregulated in astrocytes with age, are significantly upregulated in Gly-Low fed mice relative to aged controls (**Figure S4E**). These findings indicate that Gly-Low is most likely influencing hypothalamic aging signatures by preventing age-related changes that occur in the glial and immune cells of the brain. Given that these cell types are largely responsible for modulating inflammation in the brain, especially with age, the changes that Gly-Low imparts are likely to reduce generalized inflammation in the hypothalamus and potentially in other regions of the brain.

Gly-Low Rescues Aging-Associated Dysregulations in Glucose Homeostasis and Extends Lifespan

Hypothalamic aging has been shown to drive whole-body aging[39,41–44]. Therefore, we wondered if the anti-aging effects observed in the hypothalamus of Gly-Low fed mice extended more broadly and might be reflected in improved metabolism and/or lifespan. Indeed, we found that aged mice fed a Gly-Low supplemented diet beginning at 20 months of age had reduced fasting blood glucose levels, consistent with improved glucose homeostasis (**Figure 4G**). To test whether Gly-Low could influence lifespan as a late-life treatment, we began a cohort of male C57BL/6J mice beginning at 24 months of age with a Gly-Low diet. Natural lifespan and deaths were recorded, and mice were only removed from the study based on stringent health parameters. Survival analysis demonstrated that control fed mice lived a median of 825 days (105 days after beginning dietary intervention) while Gly-Low fed mice lived a median of 888 days (173 days after beginning dietary intervention) (**Figure 4H**). This represented an 8.25% increase in overall median lifespan ($p=0.0199$, Mantel-Cox), and a 5.23% increase in maximum lifespan when treatment is started at 24 months of age. Additionally, the difference in lifespan is also 60.7% increase in time survived post-intervention. This extension in both median and maximum lifespan as a late-life intervention is not observed with caloric restriction (CR), suggesting that the extension is not driven fully by reduced food intake[45,46]. This also indicates that, in addition to the health benefits of reduced calorie intake, Gly-Low is conferring benefits that allow for its ability to extend lifespan even late in life.

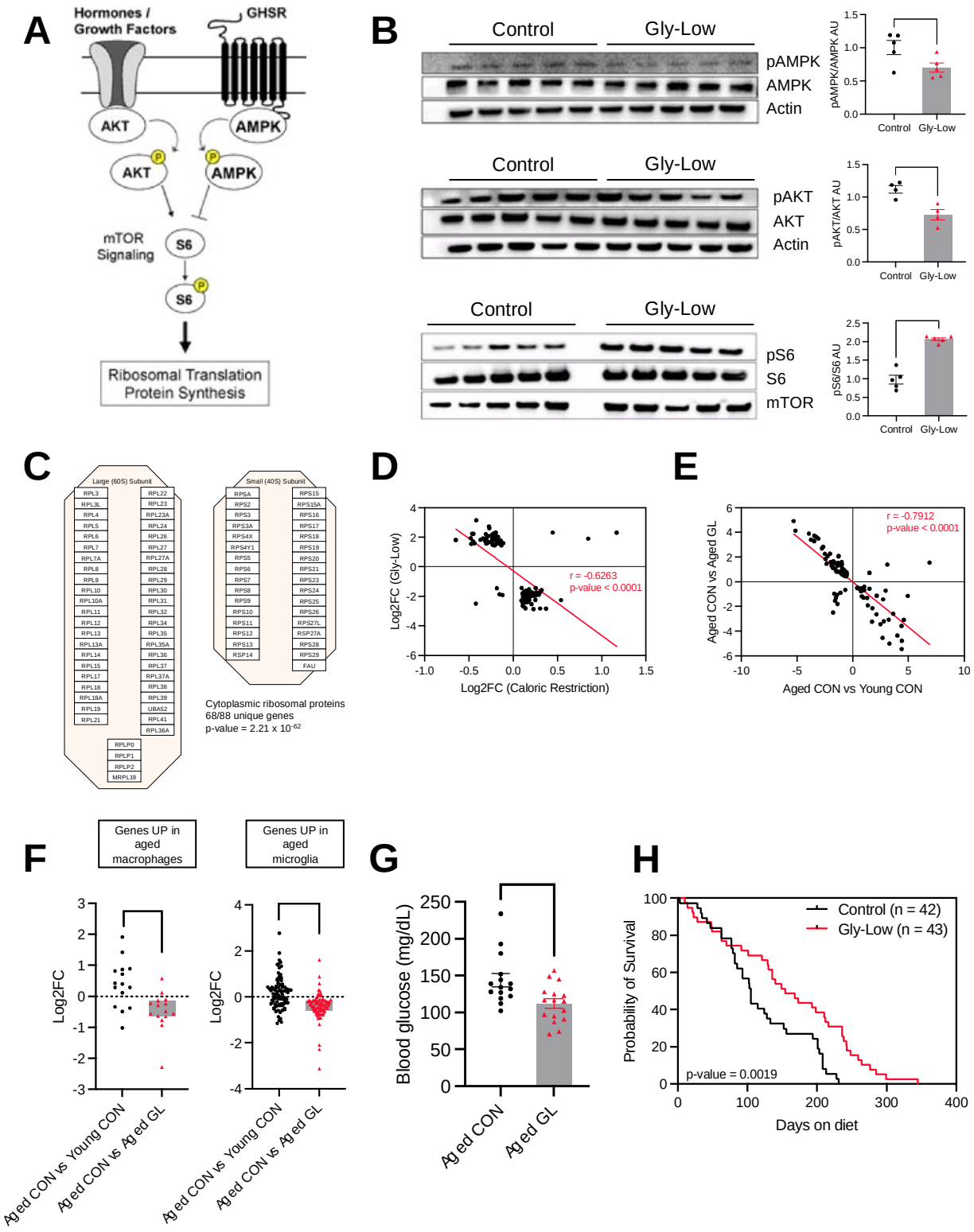
A
Hormones / Growth Factors
GHSR
AKT
AMPK
AKT
AMPK
mTOR Signaling
S6
S6
Ribosomal Translation Protein Synthesis
B
Control
Gly-Low
pAMPK
AMPK
Actin
pAMPK/AMPK AU
Control
Gly-Low
pAKT
AKT
Actin
pAKT/AKT AU
Control
Gly-Low
pS6
S6
mTOR
pS6/S6 AU
C
Large (60S) Subunit
Small (40S) Subunit
Cytoplasmic ribosomal proteins
68/88 unique genes
p-value = 2.21 x 10-62
D
Log2FC (Gly-Low)
Log2FC (Caloric Restriction)
r = -0.6263
p-value < 0.0001
E
Aged CON vs Aged GL
Aged CON vs Young CON
r = -0.7912
p-value < 0.0001
F
Genes UP in aged macrophages
Genes UP in aged microglia
Log2FC
Aged CON vs Young CON
Aged CON vs Aged GL
G
Blood glucose (mg/dL)
Aged CON
Aged GL
H
Probability of Survival
Control (n = 42)
Gly-Low (n = 43)
p-value = 0.0019
Days on diet

Figure 4: Impaired ghrelin signaling influences mTOR activation, increases ribosomal translation, and has anti-aging effects as a late-life intervention, unseen with caloric restriction. A) Schematic depicting how ghrelin signaling activates or inhibits mTOR signaling and ribosomal translation. B) Western blots of hypothalamic lysates from mice acutely (1 week) treated with Gly-Low. Protein expression of phosphorylated AMPK (top), phosphorylated AKT (middle), and phosphorylated S6 kinase (bottom) relative to their un-phosphorylated protein levels with quantification (right). C) The top regulated pathway from KEGG analysis from the 711 positive differentially expressed genes was cytoplasmic ribosomal proteins. Pink highlights the matching genes from the large and small ribosomal subunits upregulated in Gly-Low fed mouse hypothalamus. D) Fold changes in genes from a calorically restricted hypothalamus (ref 38) negatively correlate with fold changes seen in the same genes with Gly-Low treatment. E) Scatterplot showing the log2 fold changes of genes significantly altered (p value < 0.05) in the hypothalamus of aged mice (25 months) fed Gly-Low vs aged (25 months) control fed mice, plotted against fold changes of aged (25 months) control fed mice vs young (3 months) control fed mice. The regression line is shown in red. The Pearson correlation coefficient, r, is shown in the top right quadrant. F) Boxplots showing the log2 fold changes of genes that are significantly upregulated with age in hypothalamic macrophages or microglia (ref 40) G) Blood glucose levels of aged mice (25 months) treated with Gly-Low were significantly lower than those of aged control mice. H) Kaplan-Meier curve demonstrates that Gly-Low extended lifespan as a late life intervention (beginning at 24-months of age) compared to control fed mice. Significance: * p<0.05, ** p<0.005, **** p<0.00005. Statistical analyses performed by unpaired T-test.

Discussion

Here we report preclinical findings that support Gly-Low as a potential therapeutic for the treatment of obesity- and diabetes-associated pathologies. We selected the compounds that make Gly-Low based on their ability to protect against glycation stress. For that reason, we chose to initially test Gly-Low's therapeutic potential in the well-studied, glycation-burdened *Lepr*^{db} mouse model of hyperphagia and obesity[16]. As expected, Gly-Low significantly reduced systemic levels of glycation stress as measured by reduced levels of the glycation precursor, MGO, and its AGE, MG-H1. This study in mice and our previous studies in *C. elegans*, support the use of glycation lowering compounds as a therapeutic strategy against diabetic pathologies[13,47]. Methylglyoxal has been suggested as a critical target for aging and age-related diseases but has been a challenge to target this pharmacologically[47]. We demonstrate that Gly-Low reduces MGO and its glycation product, MG-H1 and that it likely does so by multiple mechanisms including lowering production via glycolysis and increasing clearance by enhancing detoxification.

In addition to Gly-Low's ability to reduce glycation stress, we found that Gly-Low had appetite-suppressing effects resulting in reduced calorie intake. Given that *Lepr*^{db} mice are glycation burdened and hyperphagic, we are not surprised to find that Gly-Low rescued many pathological phenotypes in this mouse model. However, Gly-Low also had health-promoting effects in young and aged wild-type male mice. Mechanistically, attributing Gly-Low's therapeutic effect to either its glycation-lowering capacity or its calorie-reducing effect remains a challenge. We demonstrate that these effects are happening in tandem, though it remains to be seen whether these are causative effects.

Further complicating this separation are studies that suggest a direct link between levels of glycation stress and food consumption and/or body weight. For example, feeding mice MGO-modified bovine serum albumin induced insulin resistance, increased body weight, and shortened lifespan[48]. A clinical trial in which people were given glyoxalase activating compounds, which detoxify MGO, found that these compounds reduced weight and insulin resistance [27]. These findings suggest that Gly-Low's health-promoting effects are likely due to a complex interaction between its ability to directly reduce glycation stress and directly or indirectly reduce food consumption.

The mechanism by which Gly-Low affects feeding behavior is potentially also through multiple mechanisms within the hypothalamus. Previous reports suggest that increased hypothalamic mTOR regulation and ribosomal translation increase satiety to reduce food intake in mice[49]. We observed that Gly-Low treatment impairs ghrelin responsiveness without reducing endogenous levels of active ghrelin, in part through activation of mTOR signaling. We also observed that Gly-Low increases expression of genes involved in ATP synthesis. It has been shown before that increased hypothalamic ATP and the activation of subsequent ATP-sensitive calcium channels found in dopaminergic neurons are capable of reducing food intake and preventing diet-induced obesity[50,51]. An intriguing possibility is that Gly-Low is elevating hypothalamic ATP levels, similar to the anorectic steroidal glycoside, P57AS3[50]. Elevated ATP levels are consistent with our finding that Gly-Low reduces levels of phosphorylated AMPK in the hypothalamus. Future studies are required to further elucidate the mechanisms of the impairment of ghrelin signaling. Together our data and these previously reported findings, suggest that modulation of the hypothalamus to impair ghrelin signaling leads to a voluntary caloric restriction phenotype in Gly-Low treated mice.

Consistent with our findings, previously published data on *Ghsr* null mice demonstrate reduced body weights, reduced food intake, and reduced absolute fat and lean body mass[52,53]. *Ghsr* null mice also demonstrated reduced blood glucose levels compared to wild-type mice. Interestingly, IGF-1 levels were unchanged upon depletion of the Ghsr gene, conversely to what we observed with Gly-Low treatment[52,53]. This may suggest that Gly-Low's effect is not solely through Ghsr signaling and may be impacting multiple autocrine and/or paracrine signaling cascades. This was unexplored in our current study. Limitations to this study are also imposed by findings that there are sexual dimorphisms in response to impaired ghrelin signaling[53], as our study was restricted to the use of male mice.

Caloric restriction (CR) is one of the most potent and widely conserved interventions for increasing healthspan and lifespan across species[54]. Certainly, some of Gly-Low's health-promoting effects are due in part to its calorie-reducing effect. However, in this study, we demonstrated that Gly-Low distinguishes itself from conventional CR in several ways. One important distinction between CR and Gly-Low is Gly-Low's ability to extend lifespan even when administered as a late-life treatment[45,46]; it is otherwise reported that late-life benefits of CR are titrated by the age at which it is started. A report by Lipman in 1995 demonstrates no change in median lifespan of rats fed 33% less than controls (33% CR) when treated beginning at 18 months of age[45]. Interestingly, we

demonstrate in our study that Gly-Low treatment at 24 months of age resulted in an increase in both median and maximum lifespan, with mice voluntarily eating 13.4-29.6% less than their control-fed counterparts (data not shown). We think that Gly-Low is promoting metabolic health with anti-aging effects in part through altered hypothalamic signaling, which in parallel, influences feeding behavior and whole body aging phenotypes[39,41–43]. Hypothalamic transcript analysis from aged mice fed a Gly-Low diet indicates that many genes whose expression changes with age are reversed when old mice are treated with Gly-Low. The genes that are altered suggest that glial and immune cells are the most influenced by Gly-Low treatment[40]. These changes suggest that the inflammation that occurs with age in the hypothalamus, and that is largely driven by these cell types, is rescued in aged mice fed a Gly-Low diet. Intriguingly, when we performed gene set enrichment analysis on genes whose expression changes in aged Gly-Low treated mice, we found a significant downregulation of genes involved in epithelial to mesenchymal transition (EMT). This pathway was shown to be upregulated in aged hypothalamic endothelial cells[40]. Endothelial cells are a critical component of the blood-brain barrier (BBB), which becomes compromised with age and in many neurodegenerative conditions. Although EMT is best known for its roles in cancer metastasis, it may have a role in BBB compromise that occurs with some neurodegenerative diseases[55]. Within many regions of the aging brain, including the hypothalamus, resident immune cells, macrophages, and microglia, become activated contributing to inflammatory signaling and blood-brain barrier compromise. This is likely independent of EMT and may have direct links to glycation stress. For example, MGO scavenger, aminoguanidine, has been shown to inhibit inducible nitric oxide synthase (iNOS), which mediates the activation and expansion of hypothalamic macrophages that induce activation of other glial cells, like astrocytes, and causes BBB disruption in high-fat diet fed mice[56,57]. If future studies find that Gly-Low maintains BBB integrity in aged wild-type mice, it will be interesting to test Gly-Low as a therapeutic for neurodegenerative diseases, like multiple sclerosis, in which BBB compromise serves a major role in disease progression[55].

Lowering glycation stress through glycation lowering therapies such as Gly-Low have the potential to treat many pathological conditions associated with obesity and diabetes. However, we think therapies such as Gly-Low that also induce a voluntary reduction in food consumption will show additive metabolic and health benefits. Caloric restriction (CR) has been shown to improve metabolic health and slow aging and age-related diseases in multiple species[58]. However, long-term CR is not sustainable in humans[59]. Therefore, the development of interventions that allow voluntary CR holds promise to enhance healthspan. We demonstrate, both phenotypically and transcriptionally, that Gly-Low treatment differs from CR: unlike caloric restriction, Gly-Low is quite effective at extending lifespan even late in life, which might be in part due to improved metabolic flexibility as seen by improved insulin sensitivity[46]. Thus, reducing MGO-induced glycation could serve as an effective therapeutic to improve metabolic health and slow aging and age-related diseases.

References

1. Blüher, M. (2019). Obesity: global epidemiology and pathogenesis. Nat. Rev. Endocrinol. *15*, 288–298. 10.1038/s41574-019-0176-8.

2. Popkin, B.M., Du, S., Green, W.D., Beck, M.A., Algaith, T., Herbst, C.H., Alsukait, R.F., Alluhidan, M., Alazemi, N., and Shekar, M. (2020). Individuals with obesity and COVID-19: A global perspective on the epidemiology and biological relationships. Obes. Rev. *21*. 10.1111/obr.13128.

3. Obradovic, M., Sudar-Milovanovic, E., Soskic, S., Essack, M., Arya, S., Stewart, A.J., Gojobori, T., and Isenovic, E.R. (2021). Leptin and Obesity: Role and Clinical Implication. Front. Endocrinol. *12*, 585887. 10.3389/fendo.2021.585887.

4. Yadav, A., Kataria, M.A., Saini, V., and Yadav, A. (2013). Role of leptin and adiponectin in insulin resistance. Clinica Chimica Acta *417*, 80–84. 10.1016/j.cca.2012.12.007.

5. Masuzaki, H., Tanaka, T., Ebihara, K., Hosoda, K., and Nakao, K. (2009). Hypothalamic melanocortin signaling and leptin resistance—Perspective of therapeutic application for obesity-diabetes syndrome. Peptides *30*, 1383–1386. 10.1016/j.peptides.2009.04.008.

6. Johnson, R.J., Sánchez-Lozada, L.G., Andrews, P., and Lanaspa, M.A. (2017). Perspective: A historical and scientific perspective of sugar and its relation with obesity and diabetes. Adv. Nutr. *8*, 412–422. 10.3945/an.116.014654.

7. Allaman, I., Bélanger, M., and Magistretti, P.J. (2015). Methylglyoxal, the dark side of glycolysis. Frontiers in Neuroscience *9*. 10.3389/fnins.2015.00023.

8. Schalkwijk, C.G., and Stehouwer, C.D.A. (2020). Methylglyoxal, a highly reactive dicarbonyl compound, in diabetes, its vascular complications, and other age-related diseases. Physiol. Rev. *100*, 407–461. 10.1152/physrev.00001.2019.

9. Vistoli, G., De Maddis, D., Cipak, A., Zarkovic, N., Carini, M., and Aldini, G. (2013). Advanced glycoxidation and lipoxidation end products (AGEs and ALEs): an overview of their mechanisms of formation. Free Radic. Res. *47 Suppl 1*, 3–27. 10.3109/10715762.2013.815348.

10. Bellier, J., Nokin, M.J., Lardé, E., Karoyan, P., Peulen, O., Castronovo, V., and Bellahcène, A. (2019). Methylglyoxal, a potent inducer of AGEs, connects between diabetes and cancer. Diabetes Research and Clinical Practice *148*, 200–211. 10.1016/j.diabres.2019.01.002.

11. Maessen, D.E.M., Stehouwer, C.D.A., and Schalkwijk, C.G. (2015). The role of methylglyoxal and the glyoxalase system in diabetes and other age-related diseases. Clinical Science *128*, 839–861. 10.1042/CS20140683.

12. Goldin, A., Beckman, J.A., Schmidt, A.M., and Creager, M.A. (2006). Advanced glycation end products: sparking the development of diabetic vascular injury. Circulation *114*, 597–605. 10.1161/CIRCULATIONAHA.106.621854.

13. Chaudhuri, J., Bose, N., Gong, J., Hall, D., Rifkind, A., Bhaumik, D., Peiris, T.H., Chamoli, M., Le, C.H., Liu, J., et al. (2016). A Caenorhabditis elegans Model Elucidates a Conserved

Role for TRPA1-Nrf Signaling in Reactive α-Dicarbonyl Detoxification. Curr. Biol. *26*, 3014–3025. 10.1016/j.cub.2016.09.024.

14. Hammes, H.-P., Du, X., Edelstein, D., Taguchi, T., Matsumura, T., Ju, Q., Lin, J., Bierhaus, A., Nawroth, P., Hannak, D., et al. (2003). Benfotiamine blocks three major pathways of hyperglycemic damage and prevents experimental diabetic retinopathy. Nat Med *9*, 294–299. 10.1038/nm834.

15. Voziyan, P.A., and Hudson, B.G. (2005). Pyridoxamine as a multifunctional pharmaceutical: Targeting pathogenic glycation and oxidative damage. Cell. Mol. Life Sci. *62*, 1671–1681. 10.1007/s00018-005-5082-7.

16. Guilbaud, A., Howsam, M., Niquet-Léridon, C., Delguste, F., Boulanger, E., and Tessier, F.J. (2019). The LepR $^{db/db}$ mice model for studying glycation in the context of diabetes. Diabetes Metab Res Rev *35*, e3103. 10.1002/dmrr.3103.

17. D'Agati, V.D., Chagnac, A., De Vries, A.P.J., Levi, M., Porrini, E., Herman-Edelstein, M., and Praga, M. (2016). Obesity-related glomerulopathy: clinical and pathologic characteristics and pathogenesis. Nat Rev Nephrol *12*, 453–471. 10.1038/nrneph.2016.75.

18. Sataranatarajan, K., Ikeno, Y., Bokov, A., Feliers, D., Yalamanchili, H., Lee, H.J., Mariappan, M.M., Tabatabai-Mir, H., Diaz, V., Prasad, S., et al. (2016). Rapamycin Increases Mortality in *db/db* Mice, a Mouse Model of Type 2 Diabetes. GERONA *71*, 850–857. 10.1093/gerona/glv170.

19. Kwon, O., Kim, K.W., and Kim, M.-S. (2016). Leptin signalling pathways in hypothalamic neurons. Cell. Mol. Life Sci. *73*, 1457–1477. 10.1007/s00018-016-2133-1.

20. Elizondo-Vega, R.J., Recabal, A., and Oyarce, K. (2019). Nutrient Sensing by Hypothalamic Tanycytes. Front. Endocrinol. *10*, 244. 10.3389/fendo.2019.00244.

21. Huang, Z., Liu, L., Zhang, J., Conde, K., Phansalkar, J., Li, Z., Yao, L., Xu, Z., Wang, W., Zhou, J., et al. (2022). Glucose-sensing glucagon-like peptide-1 receptor neurons in the dorsomedial hypothalamus regulate glucose metabolism. Sci. Adv. *8*, eabn5345. 10.1126/sciadv.abn5345.

22. Puskas, F. (2000). Stimulation of the pentose phosphate pathway and glutathione levels by dehydroascorbate, the oxidized form of vitamin C. The FASEB Journal *14*, 1352–1361. 10.1096/fj.14.10.1352.

23. Kammerscheit, X., Hecker, A., Rouhier, N., Chauvat, F., and Cassier-Chauvat, C. (2020). Methylglyoxal Detoxification Revisited: Role of Glutathione Transferase in Model Cyanobacterium *Synechocystis* sp. Strain PCC 6803. mBio *11*, e00882-20. 10.1128/mBio.00882-20.

24. Sohn, J.-W. (2015). Network of hypothalamic neurons that control appetite. BMB Reports *48*, 229–233. 10.5483/BMBRep.2015.48.4.272.

25. Balthasar, N., Coppari, R., McMinn, J., Liu, S.M., Lee, C.E., Tang, V., Kenny, C.D., McGovern, R.A., Chua, S.C., Elmquist, J.K., et al. (2004). Leptin Receptor Signaling in

POMC Neurons Is Required for Normal Body Weight Homeostasis. Neuron *42*, 983–991. 10.1016/j.neuron.2004.06.004.

26. Berglund, E.D., Vianna, C.R., Donato, J., Kim, M.H., Chuang, J.-C., Lee, C.E., Lauzon, D.A., Lin, P., Brule, L.J., Scott, M.M., et al. (2012). Direct leptin action on POMC neurons regulates glucose homeostasis and hepatic insulin sensitivity in mice. J. Clin. Invest. *122*, 1000–1009. 10.1172/JCI59816.

27. Cowley, M.A., Smith, R.G., Diano, S., Tschöp, M., Pronchuk, N., Grove, K.L., Strasburger, C.J., Bidlingmaier, M., Esterman, M., Heiman, M.L., et al. (2003). The Distribution and Mechanism of Action of Ghrelin in the CNS Demonstrates a Novel Hypothalamic Circuit Regulating Energy Homeostasis. Neuron *37*, 649–661. 10.1016/S0896-6273(03)00063-1.

28. Yang, Y., Atasoy, D., Su, H.H., and Sternson, S.M. (2011). Hunger States Switch a Flip-Flop Memory Circuit via a Synaptic AMPK-Dependent Positive Feedback Loop. Cell *146*, 992–1003. 10.1016/j.cell.2011.07.039.

29. Kojima, M., and Kangawa, K. (2005). Ghrelin: Structure and Function. Physiological Reviews *85*, 495–522. 10.1152/physrev.00012.2004.

30. Young Cruz, C.R., and Smith, R.G. (2007). The Growth Hormone Secretagogue Receptor. In Vitamins & Hormones (Elsevier), pp. 47–88. 10.1016/S0083-6729(06)77004-2.

31. Sun, Y., Wang, P., Zheng, H., and Smith, R.G. (2004). Ghrelin stimulation of growth hormone release and appetite is mediated through the growth hormone secretagogue receptor. Proc. Natl. Acad. Sci. U.S.A. *101*, 4679–4684. 10.1073/pnas.0305930101.

32. Ge, X., Yang, H., Bednarek, M.A., Galon-Tilleman, H., Chen, P., Chen, M., Lichtman, J.S., Wang, Y., Dalmas, O., Yin, Y., et al. (2018). LEAP2 Is an Endogenous Antagonist of the Ghrelin Receptor. Cell Metab. *27*, 461-469.e6. 10.1016/j.cmet.2017.10.016.

33. Kojima, M., Hosoda, H., Date, Y., Nakazato, M., Matsuo, H., and Kangawa, K. (1999). Ghrelin is a growth-hormone-releasing acylated peptide from stomach. Nature *402*, 656–660. 10.1038/45230.

34. Hara, M., Nishi, Y., Yamashita, Y., Hirata, R., Takahashi, S., Nagamitsu, S., Hosoda, H., Kangawa, K., Kojima, M., and Matsuishi, T. (2014). Relation between circulating levels of GH, IGF-1, ghrelin and somatic growth in Rett syndrome. Brain and Development *36*, 794–800. 10.1016/j.braindev.2013.11.007.

35. Lawrence, C.B., Snape, A.C., Baudoin, F.M.-H., and Luckman, S.M. (2002). Acute Central Ghrelin and GH Secretagogues Induce Feeding and Activate Brain Appetite Centers. Endocrinology *143*, 155–162. 10.1210/endo.143.1.8561.

36. Martins, L., Fernández-Mallo, D., Novelle, M.G., Vázquez, M.J., Tena-Sempere, M., Nogueiras, R., López, M., and Diéguez, C. (2012). Hypothalamic mTOR Signaling Mediates the Orexigenic Action of Ghrelin. PLoS ONE *7*, e46923. 10.1371/journal.pone.0046923.

37. Liu, G.Y., and Sabatini, D.M. (2020). mTOR at the nexus of nutrition, growth, ageing and disease. Nat Rev Mol Cell Biol *21*, 183–203. 10.1038/s41580-019-0199-y.

38. Liu, X., Jin, Z., Summers, S., Derous, D., Li, M., Li, B., Li, L., and Speakman, J.R. (2022). Calorie restriction and calorie dilution have different impacts on body fat, metabolism, behavior, and hypothalamic gene expression. Cell Rep. *39*, 110835. 10.1016/j.celrep.2022.110835.

39. Cai, D., and Khor, S. (2019). “Hypothalamic Microinflammation” Paradigm in Aging and Metabolic Diseases. Cell Metab. *30*, 19–35. 10.1016/j.cmet.2019.05.021.

40. Hajdarovic, K.H., Yu, D., Hassell, L.A., Evans, S.A., Packer, S., Neretti, N., and Webb, A.E. (2022). Single-cell analysis of the aging female mouse hypothalamus. Nature Aging *2*, 662–678. 10.1038/s43587-022-00246-4.

41. Zhang, Y., Kim, M.S., Jia, B., Yan, J., Zuniga-Hertz, J.P., Han, C., and Cai, D. (2017). Hypothalamic stem cells control ageing speed partly through exosomal miRNAs. Nature *548*, 52–57. 10.1038/nature23282.

42. Xiao, Y.Z., Yang, M., Xiao, Y., Guo, Q., Huang, Y., Li, C.J., Cai, D., and Luo, X.H. (2020). Reducing Hypothalamic Stem Cell Senescence Protects against Aging-Associated Physiological Decline. Cell Metab. *31*, 534-548.e5. 10.1016/j.cmet.2020.01.002.

43. Tang, Y., Purkayastha, S., and Cai, D. (2015). Hypothalamic microinflammation: a common basis of metabolic syndrome and aging. Trends Neurosci. *38*, 36–44. 10.1016/j.tins.2014.10.002.

44. Zhang, G., Li, J., Purkayastha, S., Tang, Y., Zhang, H., Yin, Y., Li, B., Liu, G., and Cai, D. (2013). Hypothalamic programming of systemic ageing involving IKK-β, NF-κB and GnRH. Nature *497*, 211–216. 10.1038/nature12143.

45. Lipman, R.D., Smith, D.E., Bronson, R.T., and Blumberg, J. (1995). Is late-life caloric restriction beneficial? Aging *7*, 136–139. 10.1007/BF03324303.

46. Hahn, O., Drews, L.F., Nguyen, A., Tatsuta, T., Gkioni, L., Hendrich, O., Zhang, Q., Langer, T., Pletcher, S., Wakelam, M.J.O., et al. (2019). A nutritional memory effect counteracts the benefits of dietary restriction in old mice. Nature Metabolism *1*, 1059–1073. 10.1038/s42255-019-0121-0.

47. Chaudhuri, J., Bains, Y., Guha, S., Kahn, A., Hall, D., Bose, N., Gugliucci, A., and Kapahi, P. (2018). The Role of Advanced Glycation End Products in Aging and Metabolic Diseases: Bridging Association and Causality. Cell Metab. *28*, 337–352. 10.1016/j.cmet.2018.08.014.

48. Cai, W., Ramdas, M., Zhu, L., Chen, X., Striker, G.E., and Vlassara, H. (2012). Oral advanced glycation endproducts (AGEs) promote insulin resistance and diabetes by depleting the antioxidant defenses AGE receptor-1 and sirtuin 1. Proc. Natl. Acad. Sci. U. S. A. *109*, 15888–15893. 10.1073/pnas.1205847109.

49. Hu, F., Xu, Y., and Liu, F. (2016). Hypothalamic roles of mTOR complex I: integration of nutrient and hormone signals to regulate energy homeostasis. Am. J. Physiol. Endocrinol. Metab. *310*, E994–E1002. 10.1152/ajpendo.00121.2016.

50. MacLean, D.B., and Luo, L.-G. (2004). Increased ATP content/production in the hypothalamus may be a signal for energy-sensing of satiety: studies of the anorectic

mechanism of a plant steroidal glycoside. Brain Res. *1020*, 1–11. 10.1016/j.brainres.2004.04.041.

51. Cowen, N., and Bhatnagar, A. (2020). The Potential Role of Activating the ATP-Sensitive Potassium Channel in the Treatment of Hyperphagic Obesity. Genes *11*. 10.3390/genes11040450.

52. Nogueiras, R., Perez-Tilve, D., Wortley, K., and Tschop, M. (2006). Growth Hormone Secretagogue (Ghrelin-) Receptors - A Complex Drug Target for the Regulation of Body Weight. CNSNDDT *5*, 335–343. 10.2174/187152706777452227.

53. Zigman, J.M. (2005). Mice lacking ghrelin receptors resist the development of diet-induced obesity. Journal of Clinical Investigation *115*, 3564–3572. 10.1172/JCI26002.

54. Green, C.L., Lamming, D.W., and Fontana, L. (2022). Molecular mechanisms of dietary restriction promoting health and longevity. Nat. Rev. Mol. Cell Biol. *23*, 56–73. 10.1038/s41580-021-00411-4.

55. Derada Troletti, C., de Goede, P., Kamermans, A., and de Vries, H.E. (2016). Molecular alterations of the blood–brain barrier under inflammatory conditions: The role of endothelial to mesenchymal transition. Biochimica et Biophysica Acta (BBA) - Molecular Basis of Disease *1862*, 452–460. 10.1016/j.bbadis.2015.10.010.

56. Leone, A., Nigro, C., Nicolò, A., Prevenzano, I., Formisano, P., Beguinot, F., and Miele, C. (2021). The dual-role of Methylglyoxal in tumor progression - novel therapeutic approaches. Front. Oncol. *11*, 645686. 10.3389/fonc.2021.645686.

57. Lee, C.H., Kim, H.J., Lee, Y.-S., Kang, G.M., Lim, H.S., Lee, S.-H., Song, D.K., Kwon, O., Hwang, I., Son, M., et al. (2018). Hypothalamic Macrophage Inducible Nitric Oxide Synthase Mediates Obesity-Associated Hypothalamic Inflammation. Cell Rep. *25*, 934-946.e5. 10.1016/j.celrep.2018.09.070.

58. Kapahi, P., Kaeberlein, M., and Hansen, M. (2017). Dietary restriction and lifespan: Lessons from invertebrate models. Ageing Res. Rev. *39*, 3–14. 10.1016/j.arr.2016.12.005.

59. Redman, L.M., and Ravussin, E. (2011). Caloric Restriction in Humans: Impact on Physiological, Psychological, and Behavioral Outcomes. Antioxidants & Redox Signaling *14*, 275–287. 10.1089/ars.2010.3253.

Methods

Mice

Studies included the use of male C57BL/6J (Jackson Laboratories #000664) control mice, male leptin receptor deficient mice (Jackson Laboratories #000642, homozygous for $Lepr^{db}$, wild type for $Dock7^{m}$) aged between 8 and 12 weeks, as well as 19-month-old male C57BL/6J mice (National Institutes of Aging, Bethesda, MD). All mice were communally housed and age-matched with *ad libitum* access to water and diet in a pathogen and temperature-controlled room with a 12h light-dark cycle beginning at 06:00 AM. All procedures were conducted per NIH Guidelines for Care and Use of Animals and were approved by the Institutional Animal Care and Use Committees at Buck Institute for Research on Aging and the University of California San Francisco.

Experimental Diets

Mice were fed either a standard low-fat chow diet (21% fat (kcal), 60% carbohydrate (kcal) Envigo: TD.200743), a standard high fat chow diet (60% fat (kcal), 21% carbohydrate (kcal), Envigo: TD.200299), a standard low-fat chow diet supplemented with our Gly-Low compound cocktail (21% fat (kcal), 60% carbohydrate (kcal) Envigo: TD.200742), or a standard high fat chow diet supplemented with our Gly-Low compound cocktail (60% fat (kcal), 21% carbohydrate (kcal).

A combination of supplemental grade compounds, safe to be consumed in set dosages, were prepared and incorporated into a modified pre-irradiated standard AIN-93G mouse chow diet from Envigo. The cocktail consists of alpha lipoic acid (20.19%), nicotinamide (57.68%), thiamine hydrochloride (4.04%), piperine (1.73%), and pyridoxamine dihydrochloride (16.36%), and is supplemented in the diet to achieve a daily consumption rate in mg/kg of body weight/day. Noted vocabulary where 1X is equal to a full dose, 0.5X is equal to a half dose, and 0.25X is equal to a quarter dose of the compound cocktail.

Lifespan

19-month-old male C57BL/6J mice received from National Institutes of Aging (Bethesda, MD) and maintained on vivarium chow until they reached 24 months of age. At 24 months of age, mice were randomly assigned to begin either a control chow diet or Gly-Low diet. Health checks were performed 5 times a week and mice reached either a humane endpoint or died of natural causes.

Measuring Food Intake and Energy Metabolism

Food consumption and body weight were measured once weekly. Chow weight of communally caged mice was recorded once weekly and individual intake was measured as change in weight over the week divided by the number of mice per cage.

Metabolic parameters in mice were assessed using a Promethion Metabolic Caging System housed in the Buck Institute Mouse Phenotyping Core. Mice were singly housed and received water and food *ad libitum*. Cages were maintained at 20°-22° C under a 12h light-dark cycle beginning at 06:00 AM, and mice were acclimated to single housing

24h before being studied. The cages continuously weighed food for each mouse, and daily intake was measured as a change in food weight over 24h periods. Metabolic data were collected by the respiration rates of each mouse and were normalized to individual mouse body mass. X, Y, and Z beam breaks quantified total activity and steps taken during the metabolic cage run.

Body Composition Quantification

Echo MRI and DXA scans were used to analyze body composition in anesthetized (isoflurane) immobilized mice. Water weight and bone mass were excluded from body weight to quantify lean and fast mass.

Glucose Testing

Random (non-fasted) and fasted blood glucose levels were determined for each mouse after 8 weeks and 16 weeks of treatment. Non-fasted blood glucose levels were assessed between 08:00 AM and 10:00 AM by a collection of blood by tail nick and the use of a handheld glucometer (AccuCheck). Fasted blood glucose was determined after a 16h fast between 8:00 AM and 10:00 AM by a collection of blood by tail nick and the use of a handheld glucometer (AccuCheck).

Glucose and Insulin Tolerance Testing

Mice underwent GTT testing at 12 months of age, following 8 months of Gly-Low treatment. Food was removed from control-fed and Gly-Low fed mice for 14 hr before testing of glucose tolerance from 6:00 PM to 8:00 AM. Mice received a single IP injection of D-glucose (2 g/kg), followed by a single tail nick to collect blood for blood glucose monitoring by handheld glucometer (AccuCheck). Total glucose AUC was measured by GraphPad Analysis.

Mice underwent ITT testing at 12 months of age, following 8 months of Gly-Low treatment. Food was removed from control fed and Gly-Low fed mice 4 hr before testing of insulin tolerance from 8:00 AM to 12:00 PM. Mice received IP injections of insulin (0.75U/kg), followed by a single tail nick to collect blood glucose monitoring by handheld glucometer (AccuCheck). Mice that had a blood glucose reading <40 mg/dL were immediately removed from the study and injected with 100 uL of 2 g/kg D-glucose. Total glucose AUC was measured by GraphPad Analysis.

Leptin Injections

Mice underwent leptin sensitivity testing at 4 months of age, following 1 month of Gly-Low treatment. Food was removed from control fed and Gly-Low fed mice 16 hr before testing of leptin sensitivity from 7:00 AM to 7:00 PM. Mice received a single IP injection of either saline vehicle or leptin (1 g/kg). Food consumption rates were collected by metabolic cage food measurements. Mice were allowed four days of rest before undergoing another single IP injection of either saline vehicle or leptin (1 g/kg) to serve as their control. Total food consumption was measured by GraphPad Analysis.

Leptin Injection and pSTAT3 Signaling

Mice underwent histological leptin sensitivity testing at 4 months of age, following 1 month of Gly-Low treatment. Food was removed from control fed and Gly-Low fed mice 16 hr before testing of leptin sensitivity from 7:00 AM to 7:00 PM. Mice received a single IP injection of either saline vehicle or leptin (1 g/kg). Within 30 min of receiving the injection, mice were euthanized by CO_2 asphyxiation and cervical dislocation. Dissections were performed and mouse brains were removed and washed with PBS before being postfixed in 4% PFA overnight with agitation at 4C. Afterward, a brain matrix (BrainTree) was used to isolate sections containing the hypothalamus. This section was immediately embedded in OCT, frozen on dry ice, and stored at -80C. Next, 4-micron sections were cut on a cryostat, blocked for 1 hr with 5% BSA containing 0.1% triton X-100, and incubated with pSTAT3 (1:200, Cell Signaling). Adequate secondary antibody was used for the HRP-diaminobenzidine reaction. The HRP-diaminobenzidine reaction was performed using the ABC Kit (Vector Laboratories), using biotin-labeled goat anti-rabbit IgG. Images were acquired using a Zeiss AxioImager brightfield microscope.

Ghrelin Responsiveness

Ghrelin peptides (Catalog #031-30)(Phoenix Pharmaceuticals, Inc.). Mice were injected with reconstituted ghrelin (0.1 mg/kg) by subcutaneous injection. Following injection, mice were singly housed, and individual food consumption was recorded over 90 minutes post-injection.

Hormone Quantification:

Blood samples were collected by cardiac puncture when mice were euthanized for dissection. Blood samples were collected in heparin lined tubes and left on ice for 30 min. Afterward, samples were centrifuged for 15 min at 2200 g to isolate plasma. Ghrelin, LEAP2, and IGF-1 were measured in plasma by ELISA kits according to manufacturer's instructions.

LEAP2 ELISA (Catalog #075-40) (Phoenix Pharmaceuticals, Inc.)
Ghrelin ELISA (EZRGRA-90K)(Sigma Aldrich)
IGF-1 ELISA (Catalog #80574) (Crystal Chem)

Hypothalamic RNA Sequencing:

Hypothalamic transcripts were analyzed from male C57BL/6J mice at three ages under different treatment paradigms: 1) young (4-month-old) male C57BL/6J mice fed a control or glycation-lowering (Gly-Low) diet for 1 week, 2) aged (25-month-old) male C57BL/6J mice fed a control or glycation-lowering (Gly-Low) diet for 5 months and 3) young (3-month-old) male C57BL/6J mice fed a control diet for 1 week. Aged 19 month-old male C57BL/6J mice were ordered from the National Institutes of Aging (Bethesda, MD). Young mice were acquired from Jackson laboratories (#000664). Mice were fed vivarium chow (Envigo Teklad 2018) before starting either a control diet or Gly-Low diet. Mice were sacrificed via CO_2 asphyxiation followed by cervical dislocation. The brain was rapidly dissected and the hypothalamus was removed with tweezers, flash-frozen, and stored at -80˚C. RNA was isolated using Zymo research quick RNA miniprep kit (cat # 11-328) according to the manufacturer's recommendations. Isolated RNA was sent for library preparation and sequencing by Novogene Corporation Inc. where RNA

was poly-A selected using poly-T oligo-attached magnetic beads, fragmented, reverse transcribed using random hexamer primers followed by second strand cDNA synthesis using dTTP for non-directional library preparation. Samples underwent end repair, A-tailing, adapter ligated, size selected, amplified, and purified. Illumina libraries were quantified using Qubit and qPCR and analyzed for size distribution using a bioanalyzer. Libraries were pooled and sequenced on an Illumina Novoseq 6000 to acquire paired-end 150 bp reads. Data quality was assessed and adaptor reads and low quality reads were removed. Reads that passed the quality filtering process were mapped paired-end to the reference genome (GRCm38) using Hisat2 v2.0.5. featureCounts v1.5.0-p3 was used to count reads that mapped to each gene. Differential expression analysis was performed using DESEq2 (1.20.0). Where indicated, bootstrapping was performed using R (R version 4.1.2) program 'boot' (1.3-28.1). To determine the expected mean and standard deviation, n=i log2 fold changes were randomly selected 1000 times, in which i is the number of genes in the gene set.

Metabolomics:

Samples were prepared and analyzed by Norwest Metabolomics Research Center according to the following:

LC-MS Conditions: *Acquisition Mode MS1*; threshold count: 100; *m/z* 60-1000; Gas temp 325°C; Drying Gas 10L/min; Nebulizer 35 psi; TOF Fragmentator 120 V; Skimmer 65 V; 4 spectra/s; 250 ms/spectrum; *Acquisition Mode MS2:* range *m/z* 20-1000; 4 spectra/s; 250 ms/spectrum; CE 20 eV; 5 precursor per cycle, MS2 threshold 200 counts; active exclusion after 3 spectra; static exclusion rang m/z 60-100; Abundance dependent accumulation target 50000 counts/spectrum; exclusion list from blank injection enabled; reference mass correction enabled.

LC System: Agilent 1260 as the Mobile Phase (pump 2) and reference solution (pump 1)

MS System: Agilent 1200 SL LC-6520 Quadrupole-Time of Flight (Q-TOF) MS

LC column: WATERS XBridge BEH Amide (15 cm x 2.1 mm; 2.5 µm)

Buffer A: 10 mM ammonium acetate and 0.2% acetic acid in 95% H_2O + 3% ACN + 2% MeOH;

Buffer B: 10 mM ammonium acetate and 0.2% acetic acid in 5% H_2O + 93% ACN + 2% MeOH;

Injection: 5 µL (+)-ESI and 10 µL (-)-ESI; **Wash:** 95%ACN+5%H_2O for 10 s; **flow rate** (mL/min): 0.3

LC Column Chamber Temp: 40° C; **ESI mode:** (+/-)

Worklist: each sample was injected in both positive and negative ESI mode (labeled _POS and _NEG). Blank of sample preparation labeled as blank_Prep. Plasma and tissue samples were combined to make QC samples from plasma (QCp) and tissue (QCt).

Gradient operation (Separation)

min	B%
0	95
3	95
8	50

12	50
13	95
35	95

Plasma sample preparation:
Samples were thawed at 4°C, vortexed 10 seconds. 28uL plasma plus 22uL water was transferred to a 2 mL Eppendorf vial. 250uL Methanol was added then the sample was vortexed 10 seconds. Samples were incubated at -20˚C for 20 minutes and centrifuged at 14000 rpm at 4˚C for 15 minutes. 150uL supernatant was transferred to a new 2 mL Eppendorf vial and dried completely using a Vacufuget at 30˚C for about 1.5 hours. Samples were reconstituted with 250uL HILIC solvent, vortexed 10 seconds then centrifuged for 5 min at 14000 rpm at 4˚C. 250uL supernatant was transferred into LC vials for MS analysis.

Data processing:
Data processing was performed using Progenesis Qi software v. 2.2.5826.42898 (Nonlinear Dynamics; Newcastle; UK). Peak alignment was carried out taking samples as reference. Peak-peaking was performed using sensitivity and chromatographic peak width at 1 (3 for (+)-ESI) and 0.01min; respectively. The retention time limit was set 1.0 – 12.0 min. Possible adduct ions were defined as follows: $[M+H]^+$; $[M+Na]^+$; $[M+NH_4]^+$; $[M+K]^+$; $M^{+\bullet}$; $[M+ACN+H]^+$; in (+) ESI mode; and $[M–H]^–$; $[M+HCOO–H]^–$; $[M+Cl]^–$; and $[2M+CH3COO–H]^–$ in (-) ESI mode. The adduct ions were grouped into mass features through peak deconvolution. Putative peak annotation was performed by searching metabolites from MONA Database (https://mona.fiehnlab.ucdavis.edu/) using accurate *m/z*measurements from the full scan data and MS2 spectra. We set the *m/z* tolerance of 20 ppm (MS1) and 30 ppm (MS2).

Liver Histology:
Dissections were performed and mouse livers were removed and washed with PBS before being postfixed in 4% PFA overnight with agitation at 4C. Afterwards, livers were moved to 70% EtOH before being paraffin embedded and sectioned. The liver was sectioned by microtome in a coronal orientation at a thickness of 4 microns. H&E staining and trichrome staining were used for the identification and quantification of large lipid vacuoles.

RT-PCR:
Total RNA was extracted using Trizol (Invitrogen), purified with RNeasy Mini-Kit (Qiagen) according to manufacturer's instructions, and reverse transcribed using iScript Reverse Transcription Supermix (BioRad). cDNA was subjected to PCR analysis with gene-specific primers in the presence of SyGreen Blue Mix (Genesee). Relative mRNA abundance was obtained by normalization to actin and tubulin housekeeping genes.
Primer sequences:
Pck1 forward: (5' to 3') TGA TGA CTG TCT TGC TTT CG
Pck1 reverse: (5' to 3') GCA TAA CGG TCT GGA CTT CT
G6p forward: (5' to 3') ATA GTA TAC ACC TGC TGC GCC
G6p reverse: (5' to 3') GAT TGC TGA CCT GAG GAA CG

Western Blotting:
Proteins were extracted from hypothalamic samples in TPER buffer (Thermo Fisher) containing a protease inhibitor cocktail (Sigma). Protein extracts were denatured at 70°C for 15 min prior to running on a 5-12% Bis-Tris gel. The transfer was completed using iBlot (Thermo Fisher) and blocked in 5% BSA for 1 hr. Primary antibodies were incubated overnight at 4°C with agitation. Adequate HRP-conjugated antibodies were incubated at room temperature for 1 hr prior to imaging.
Akt (Cell Signaling)(40D4) 1:1000
pAKT Ser473 (Cell Signaling)(D9E) 1:1000
S6: (Cell Signaling) (5G10) (2217) 1:1000
pS6 Ser 240/244: (Cell Signaling) (D68F8) 1:1000
AMPK: (Cell Signaling) (CST-4181) 1:1000
pAMPK: (Cell Signaling) (CST-2531)
mTOR: (Cell Signaling) (7C10): 1:1000
Actin (Cell Signaling) (13E5) 1:1000

Mass Spectrometry MGO Quantification:
Quantification of Dicarbonyls. 200 µL of 80:20 MeOH:ddH_2O (-80°C) containing 50 pmol $^{13}C_3$-MGO was added to 10 µL of serum and extracted at -80°C overnight. Insoluble protein was removed via centrifugation at 14,000 x g for 10 min at 4°C. Supernatants were derivatized with 10 µL of 10 mM o-phenylenediamine for 2 h with end-over-end rotation protected from light (Galligan et al., 2018). Derivatized samples were centrifuged at 14,000 x *g* for 10 min and the supernatant was chromatographed using a Shimadzu LC system equipped with a 150 x 2mm, 3µm particle diameter Luna C_{18} column (Phenomenex, Torrance, CA) at a flow rate of 0.450 mL/min. Buffer A (0.1% formic acid in H_2O) was held at 90% for 0.25 min then a linear gradient to 98% solvent B (0.1% formic acid in acetonitrile) was applied over 4 min. The column was held at 98% B for 1.5 min and then washed at 90% A for 0.5 min and equilibrated to 99% A for 2 min. Multiple reaction monitoring (MRM) was conducted in positive ion mode using an AB SCIEX 4500 QTRAP with the following transitions: *m/z* 145.1→77.1 (MGO); *m/z* 235.0→157.0 (3-DG); m/z 131.0→77.0 (GO); m/z 161.0→77.0 (HPA); m/z 148.1→77.1 ($^{13}C_3$-MGO, internal standard).
Quantitation of PTMs (QuarkMod). Protein pellets from the dicarbonyl quantifications (above) were resuspended in 65 µL of 50 mM NH_4HCO_3, pH 8.0. Samples were spiked with 10 µL of a master mix containing internal standards (see table). Proteins were digested via the addition of 5 µL of sequencing grade trypsin (0.1 mg/mL) (Promega) for 3 h at 37 °C. Trypsin was denatured via boiling at 95 °C for 10 min and samples were cooled to room temperature. Aminopeptidase M (Millipore, 15 µg in 10 µL) was added and samples were incubated overnight at 37°C. Aminopeptidase was denatured via heating at 95 °C for 10 min and samples were again cooled to room temperature. 15 µL of heptafluorobutyric acid (1:1 in H_2O) was added to each sample and debris was removed via centrifugation at 14,000 × *g* for 10 min. Clarified supernatants were chromatographed using a Shimadzu LC system equipped with a 150 x 2.1mm, 3.5 mm particle diameter Eclipse XDB-C8 column (Agilent, Santa Clara, CA) at a flow rate of 0.4500 mL/min. Mobile phase A: 10 mM HFBA in water; mobile phase B: 10 mM HFBA

in ACN. The following gradient was used: 2 min, 1% B; 6 min, 50% B; 6.5 min, 95% B; 9 min 95% B; 9.5 min, 1% B. The column was equilibrated for 3 min at 5% B. MRM was conducted in positive mode using an AB SCIEX 4500 QTRAP. The MRM detection window was 50 sec with a target scan time of 0.75 sec. The following parameters were used for detection and as previously described (Gaffney et al., 2020; Galligan et al., 2017):

Species	**Q1 (*m/z*)**	**Q3 (*m/z*)**	**CE (V)**
Lys	147.1	84.1	29
$^{13}C_6{}^{15}N_2$ Lys	155.1	90.1	29
Arg	175.1	70.1	47
$^{13}C_6{}^{15}N_4$ Arg	185.1	75.1	47
Leu	132.1	86.1	17
$^{13}C_6{}^{15}N$ Leu	139.1	93.1	17
MG-H1	229.2	70.1	53
^{13}C-MG-H1	230.2	70.1	53
CEA	247.2	70.1	55
^{13}C-CEA	248.2	70.1	55
CEL	219.2	84.1	41
CEL-d_4	223.2	88.1	41
CML	205.0	84.1	38
CML-d_4	209.0	88.1	38

Quantification of free MGH1. 10 µL of serum was added to 200 µL of 80:20 MeOH:ddH_2O (-80°C) containing 10 pmol ^{13}C-MG-H1 and extracted at -80°C overnight. Insoluble protein was removed via centrifugation at 14,000 x g for 10 min at 4°C and supernatants were transferred to a new tube. 15 µL of heptafluorobutyric acid (1:1 in H_2O) was added to each sample and debris was removed via centrifugation at 14,000 × *g* for 10 min. Samples were analyzed as described above (QuARKMod).

Quantification and statistical analysis:

Statistical details of experiments can be found in the figure legends. All data are expressed as mean ± SEM as indicated in the figure legends. Statistical tests were selected based on appropriate assumptions with respect to data distribution and variance characteristics. For normally distributed data, statistical significance was determined using unpaired T test. For data normalized to the vehicle control group, statistical significance was determined using one-sample T test. All statistical analyses were performed using GraphPad Prism. Significant differences are indicated as follows: * $p \leq 0.05$, ** $p \leq 0.005$, *** $p \leq 0.0005$, **** $p < 0.0001$.